In-belt vibration monitoring of conveyor belt idler bearings by using wavelet package decomposition and artificial intelligence

Willem Abraham Roos[1,*], Philippus Stephan Heyns[1]

[1] Department of Mechanical and Aeronautical Engineering, University of Pretoria, South Africa

[*]Corresponding Author: Willem Abraham Roos; willem.roos@up.ac.za

Abstract

Conveyor belt systems generously employ idlers that support the belt and its payload as it is circulated. Visual and acoustic methods are commonly used to identify faulty or failing idler bearings but these methods can become tedious and time consuming in practice. While vibration monitoring might look like an obvious choice to explore, the instrumentation of individual idler bearings would be prohibitively expensive. The potential for using an accelerometer that moves with the belt while tracking the condition of all bearings encountered along the way is therefore potentially interesting. This possibility is explored in this work on a laboratory scale test rig. Wavelet package decomposition is used to extract the bearing features and present it to an intelligent decision making system. Artificial neural networks and support vector machines are used to identify and classify faulty idler bearings. The system could not only identify faulty bearings but also classify the faults accurately. Using a simple data acquisitioning system would amount to costs of the order of one meter of steel reinforced rubber belt. While some important practical issues such as data harvesting, downloading of the data and robustness of the system still need to be practically resolved, this work seems to indicate that a belt mounted idler monitoring system might not only be feasible but affordable as well.

Keywords

Artificial intelligence; vibration transmissibility; conveyor; idler bearing vibration monitoring; in-belt; condition-based monitoring

1. Introduction

Conveyor belts are critical to the operation of many materials handling plants in the mining industry. Conveyor belts are prone to damage when the supporting idlers seize or have difficulty rotating due to bearings failing mechanically or being contaminated with dust and dirt. In general engineering applications, it has been found that between 7,400 and 16,392 bearings can be found per kilometer of conveyor (Goodman Conveyor, n.d.). Some conveyors can be several kilometers long, resulting in thousands of bearings that could potentially fail. It is also known that most belt failures are due to idler failures (Zimroz & Król, 2009), (Kinder, 2013). According to an early feasibility study done at a power utility in South Africa there has long been a need for a system that can monitor the idlers of conveyor belts (van Tonder, 2002) but it needs to be financially competitive over its lifecycle, when taking capital, running and labour expenses into account.

A few methods have been employed to monitor the conditions of conveyor idlers; manual inspection, thermal cameras, and acoustic sensing equipment. Manual inspection entails operators walking the length of the conveyor and listening and looking for faulty idlers. It is difficult to determine the severity of an idler's fault or how urgent its replacement is based on manual inspection. Some parts of a conveyor may be difficult or dangerous to access and

could cause faulty idlers to be missed during inspection. Thermal cameras offer a great way of identifying faulty idlers (Maras, 2013). Bearings that are starting to fail will normally run slightly hotter than the other bearings. These temperature differences can easily be seen on a thermal image and help to identify faulty idlers. Acoustic equipment are used to identify audible and inaudible noise. Specialized acoustic equipment can be used to identify small deviations in bearing vibrations and serve as a fault identifier (SKF, n.d.). The acoustic equipment can identify a faulty idler bearing from 3 meters away, even when the inspector walks at a pace of 2 km/h (SKF, n.d.). These methods are however still labour intensive and raise the question of alternatives.

The vibration responses of operating mechanical equipment can reveal its condition and vibration analysis is a very commonly used tool in fault diagnosis (Li, et al., 2013). The key to vibration analysis is extracting and trending fault features that are sensitive to the relevant failure mechanisms (Li, et al., 2013). In their study Li, et al. (2013) considered the vibrations of the idlers and identified which of the idlers close-by are failing. The vibrations of three idler sets were captured by an accelerometer placed on the supporting structure of the conveyor. By applying a wavelet package decomposition to the signals and using a radial base function support vector machine a 91.67% accurate classification was made (22 of 24 datasets). Although this is a very common and time trusted monitoring method, the number of accelerometers needed to monitor an entire conveyor is far too many and the cost of such a system is probably too much to justify (Li, et al., 2013).

Unscheduled down-time of a facility due to failed conveyor idlers can lead to loss of production resulting in large monetary losses. Permanent employment of operators to manually inspect all the idlers along the length of the conveyor becomes costly as well. A trustworthy, cost-effective, automated conveyor idler monitoring system could prevent unscheduled down-time by informing operators ahead of time of critical conveyor idlers and composing a summary of other idlers that are not critical yet but could be replaced during the next planned maintenance as a preventative measure. The number of permanent operators required for the upkeep of the conveyor can be reduced as manual inspection would not be necessary anymore.

Investigating the feasibility of placing an accelerometer (or a few accelerometers spaced over the width of a conveyor belt) and the associated data acquisitioning equipment imbedded in (or on) the moving conveyor belt, and having the sensor(s) monitor the vibrations of each idler it passes is therefore the objective of this study. If this method is found to be feasible, further research and development can be done to produce a more cost-effective on-line monitoring system that could prevent unscheduled down-time and reduce the number of required conveyor operators. While the idea of placing the data acquisitioning equipment in the conveyor belt has been contemplated (Freeman, 2010), a comprehensive study into the feasibility of the idea has not been published in the open literature. Such an experimental investigation is the main contribution of the current work. The investigation would indicate whether idlers' bearing vibrations could in fact be transmitted through the idlers themselves as well as a moving conveyor belt and measured by an accelerometer attached to the belt. This was the most concerning aspect of the monitoring system - *whether the idler bearing vibrations could be transmitted to the accelerometer and not be dampened by the belt and obscured by the noise and dynamics of an operational conveyor.* The investigation would also indicate whether conveyor idler bearing fault identification can be done on the measured signals to not only identify a faulty idler, but also classify the fault.

2. Vibration transmissibility through rubber belt

The later stages of bearing failure can be detected in the frequency range associated with the bearing components like the race pass frequencies and the roller element frequencies also known as the bearing fault frequencies (Graney & Starry, 2012). The fundamental fault frequencies are considered low frequencies as they usually appear between 0.33 and 0.5 times the bearing's rotational speed (Graney & Starry, 2012). Equipment that are capable of

measuring high frequencies are usually more expensive than low frequency monitoring equipment. This contributed largely to the decision to focus on later stages of bearing failure.

The biggest concern about placing accelerometers in or on the rubber belt is the potentially low transmissibility of the vibrations from the bearings, through the idler body and the rubber belt to the sensor. To better understand the challenges due to this effect, a simple experiment was conducted before commencing with the study. This was done to investigate if it is possible to measure the vibrations through the rubber belt at various distances from the source.

- A section of steel cord reinforced conveyor belt was cut out and mounted on a fixed post at one end and attached to a servo-hydraulic actuator at the other end as seen in Figure 1. This belt is produced for the materials handling industry.
- A frequency sweep was subsequently done from 0Hz to 1000Hz with a hydraulic actuator. This range was chosen because, at this stage in the investigation, it was unknown at which frequencies bearing faults would appear. However, the investigation is aimed at low frequencies as this is where later stages of bearing failure occurs (Graney & Starry, 2012) and an upper limit of 1000Hz was chosen.
- An accelerometer was attached to the actuator piston to measure the vibration input to the belt (in this case representative of bearing idler excitation).
- An output response sensor was used to measure vibrations on the centreline on top of the belt section. The sensor was initially placed over the vibration source (as seen in Figure 1) and was then moved laterally towards the fixed mount in 50mm increments up to a distance of 400mm away from the source. 800mm is the typical distance between two idlers.
- Some mass was attached to the belt to provide some gravitational preload on the belt, in accordance with the expected effects of a payload on the belt.
- The total distance between the fixed and excited end was 800mm.

The transmissibility as function of the distance away from the source could be calculated. The transmissibility T for a given frequency f is given by the ratio of the magnitude of the Fourier transform of output M^o and the input M^i as shown in equation 1. Figure 2 shows the gradient filled contour plot of the transmissibility of vibrations through the belt.

$$T_n = \frac{\left|M^o{}_f\right|}{\left|M^i{}_f\right|} \qquad \text{(Eq. 1)}$$

As seen in Figure 2, the vibration displacement transmissibilities over the frequency range 0 – 200 Hz typically ranges between 50% and 150% . At frequencies beyond 200 Hz it is clear that the transmissibility drops significantly (with the occasional exception which is probably caused by resonance of the belt as it was supported in the test setup) and it is clear that bearing excitation will not be transferred to the sensor in the belt. This has significant implications for any belt based system and implies that one should focus on diagnostic frequencies in a range of up to typically 200 Hz. Higher frequencies could be expected to simply not transfer well enough into a belt based system. At first the bearing fundamental frequencies were not known and to ensure a large range of frequencies were investigated, it was decided to measure up to 1 kHz. As discussed later, the fundamental frequencies are in the range of 20 to 50 Hz for the chosen operating parameters, and from the transmissibilities it seems that good transfer will occur in this range for some distance from the source. The ability to sense vibrations from as far away as about 400 mm is also very important, bearing in mind that the system must capture the characteristic frequencies of each bearing it passes typically during the period that it takes the belt to traverse

about 800 mm. The experiment seems to indicate that diagnostic information could be captured over this entire distance.

3. Measuring idler vibration and classifying bearing faults

3.1. Test bench

A conveyor test bench was constructed to investigate a more realistic representation of the vibrations associated with the bearings in an idler and the different faults found in such a bearing. Figure 3 shows the test bench which comprises two larger diameter pulleys of width 200 mm, one of which is driven. The motor is powered by a variable speed drive which gives great control over the start-up and operational speeds. The rotational speed for all the tests reported here was kept more or less constant with small speed variations of the order of less than 5%. This was confirmed with a handheld tachometer. The idler was positioned a bit higher than normal to cause a downwards force simulating the payload and pre-tensioning of the conveyor. The test bench has tensioners on the main pulleys that are used to provide and control tension and align the belt.

The test bench was designed so that the data acquisitioning equipment could be installed on the outside surface of the belt, to avoid the practical problem of embedding the system in the belt for the purposes of this exploratory investigation. This was also required so that the sensor position relative to the faulty bearing could be varied to investigate the influence of the sensor placement on the system accuracy. Only one idler is used here to simplify the test bench and the data processing. Bearing in mind the requirement for low cost and the need to design something that will anyway have to be purposely packaged to fit into a specially spliced test section, a simple data logger was specifically developed (although the packaging issue was not yet addressed in this version). The data logger was built with a Teensy 3.2 micro controller. This data logger can be seen in Figure 4. The Teensy 3.2 has a clock speed of 96 MHz and with an LSM6DS33 6-DOF system-package accelerometer it reached sampling frequencies of up to 1 kHz with 16 bit resolution and up to a range of ±16g. The LSM6DS33 accelerometer has a built-in anti-aliasing filter. The logger has an SD card module that allows the accelerometer data and timestamp to be stored on an SD micro card of up to 64 Gb. The data logger has a Lithium-polymer battery built in that enables the continuous data logging for over 50 hours. The overall cost of this data logger is of the same order as 1 meter of steel reinforced rubber belt. This illustrates that such a system could be financially feasible.

3.2. Pre-processing

Figure 5 depicts an acceleration signal as measured on the belt during a single idler pass after it has been filtered with a moving average. There is a change in the sign of the acceleration measured by the sensor as it moves from the bottom to the top of the test bench. These changes are used as triggers in the current setup, and the section of the vibration signal is extracted when the sensor is on top of the belt and close to the bearing. The large spike in the middle of the signal is caused by the sudden change in vertical direction of the sensor as it passes the idler - negative vertical acceleration. There is a noticeable belt hop that is present between the pulleys and the idler and can be seen as the higher amplitude waves in the signal. Each pass of the idler will be used as a separate dataset.

As each idler is monitored on its own, each idler's signal needs to be analyzed on its own. A time domain localization can be used to focus on each idler individually. The wavelet transform (WT) has been used with success to process bearing frequencies for fault identification and classifying (Li, et al., 2013). A level 7 wavelet package decomposition (WPD) was therefore performed on all the bearing time domain data sets. Quadrature mirror filters were used as low- and high-pass filters for the wavelet package decomposition seeing that these filters have been used before with success to process bearing frequencies for fault identification and classifying (Ocak, et al., 2007).

An energy value representing each of the wavelets was calculated. This was done by calculating the sum of squares of the frequency magnitudes of each wavelet and determining the percentage contribution to the signal's total energy. The non-dimensionalized energy values are still good representations of the frequency spectrum that, in essence, represents the original signal.

3.3. Artificial intelligence systems

Artificial neural networks (ANN) and support vector machines (SVM) have previously been used in the identification and classification of bearing faults on conveyor systems (Li, et al., 2013). These two classification methods are very accurate if trained well. In this work the two systems are compared to one another to identify the more accurate and reliable system.

3.3.1. Artificial neural networks

Artificial neural networks mimic the way the human brain works. Figure 6 show a schematic of a neural network. As seen in Figure 6, there are inputs to the neural network (denoted by x), and each input is connected to neurons (denoted by z), and these neurons may be connected to other neurons and eventually some neurons are connected to outputs (denoted by y). The connections are illustrated with the solid lines. In Figure 6, there is only one hidden level - one level of neurons between the inputs and outputs. Depending on the complexity of the neural network that one wants to use, the number of hidden levels can be increased as well as the number of neurons in each hidden level. Not all hidden levels have to have the same number of neurons (Bishop, 2006). The tendency is that each input is connected to each of the neurons in the neighbouring hidden level, and then each of those connected to each neuron in the next hidden level as seen in Figure 6 (Bishop, 2006). Equation 2 shows how the input of each neuron in the first level, $Z^{(1)}{}_{N}$, is connected to each of the neural network inputs, x_i, and weighted with the first level weights $\omega^{(1)}{}_{Ni}$. The same methodology is applied in the levels that follow. Cases do exist where an input might not be connected to every neuron in the neighbouring hidden level or may even connect to a neuron in a hidden level one over. It is the weights between the inputs, neurons and outputs that are adjusted when the neural network is trained to best predict the outputs depending on the inputs. The inputs and neurons denoted by x_o and z_o are usually constants called biases and are normally set to 1 as the weighting on each connection will adjust the magnitude of the bias (Bishop, 2006).

$$Z^{(1)}{}_{N,\ N=1\ to\ M} = \sum_{i=0}^{D} x_i \times \omega^{(1)}{}_{Ni} \qquad \text{(Eq. 2)}$$

There are several ways of training a neural network by adjusting the weights between the inputs, neurons, and the outputs. The one way of adjusting the weights is to manually alter the weights and analyzing the outputs and adjusting some more as needed until the success of the neural network is satisfactory. Another way is to randomize the weights and adjusting the range of the randomization algorithm until the output is satisfactory. These methods can take quite some time to find the ideal combination of weights that will take inputs and accurately estimate the outputs.

Another way of finding the weights is by a method called gradient based back propagation. Gradient based back propagation is a method where the weights are calculated automatically. Initial weights are chosen at random and the inputs are used to produce outputs based on these initial weights. The calculated outputs of the neural network are then compared to the target outputs needed for the set of inputs. The outputs' dependencies on the different neurons connected to them, are calculated. The differences between the calculated and the target

outputs are then taken and the local gradient is calculated. The weights of the connections feeding into the output are then adjusted by the local gradient. The weights between hidden levels are adjusted in the same way. The more a connection's weight contributes to the error, the more it is adjusted to minimize the error of the neural network. These adjustments can be done for a set number of iterations or until a small enough error is made. It has been found that back propagation gives the greatest accuracy and numerical efficiency (Bishop, 2006). It is for this reason that a gradient based back propagation neural network was used to identify and classify the bearing faults in the idler.

A level 7 wavelet package decomposition was used to decompose the vibration signals into 2^7 wavelets and the non-dimensionalized energy values of each decomposed wavelet calculated. The energy values of the first 15 wavelets were used as inputs to the neural network seeing that the remaining wavelets contributed very little to the total energy of the signal. The bearing's fundamental frequencies, as discussed later, were all found within the frequency range covered by the first 15 wavelets - approximately 120 Hz. Only one hidden level was used with 25 neurons. A single output produced a value between 0 and 1 and based on pre-defined ranges could be used to classify the underlying bearing fault.

3.3.2. Support vector machines

Support vector machines are popular for solving problems in classification, regression and novelty detection (Bishop, 2006). A Support vector machine is a classifier where data sets are separated into classes. The basic support vector machine is the two-class classification problem using a linear model in a 2D feature space (Bishop, 2006). The objective of a support vector machine is to classify data to certain areas. Assuming that the support vector machine is working in a 2D feature space with a linearly separable data set, the support vector machine will separate the classes of the data set with a linear line and will also maximize the distance between the line and the closest data points of either class as a constrained optimization problem (Bishop, 2006).

Figure 7 illustrates a data set in 2D feature space that can be separated linearly. The red line is separating the two classes and is also called the decision boundary. The margin is defined as the perpendicular distance between the decision boundary and the closest data points of both classes. The margin is represented as the space between the blue lines in Figure 7. The purple circles are the data points of both classes that are closest to the decision boundary and lie on the margin. These data points are called the support vectors seeing that vectors perpendicular to the decision boundary can be drawn to each of these data points and all the vectors have the same maximum magnitude. It is these vectors that are maximized by solving the optimization problem. The rest of the data points of each class are found on either side of the margin.

It might happen that for a 2D data space, the data set cannot be separated linearly. To be able to classify these data sets, the support vector machine makes use of a non-linear kernel function that enables the data sets to be linearly separable in a non-linear feature space (Bishop, 2006). Figure 8 shows a data set in a 2D feature space (x-y plane) that has been classified by a non-linear kernel function. The contour lines represent values of the same height (z-direction). A kernel function has been applied to the x-y coordinates of the data set and a z-value (height) obtained for each data point. The data points can now be represented in 3D space and can be separated by a linear plane. It can be seen in Figure 8 that the data set is separated into two classes by a non-linear contour line. The data points marked with green circles are the support vectors.

As with the artificial neural network, the energy values of the first 15 wavelets were used as inputs to support vector machine. The data points existed in 15D feature space. Linear, polynomial, and radial base functions were used as the kernel function but the radial base function was the most accurate. Unlike the artificial neural network

that produces a value within a range that still has to be interpreted to classify the bearing fault, the support vector machine explicitly identifies the class to which the underlying bearing fault belongs to.

3.4. Validate theoretical fundamental frequencies

A bearing has a few fundamental frequencies associated with its components within. There are a number of components in a bearing that can fail, each having a different outcome on the frequency spectrum, and for this reason, different bearing fault cases were tested on the conveyor test bench. There are five bearing conditions that were tested:

- Healthy bearing.
- Outer raceway pit as seen in Figure 10. Pits forming in the surfaces of bearing raceways and rolling elements are very common bearing faults that occur.
- Inner raceway pit as seen in Figure 11.
- Rolling element pit as seen in Figure 12.
- Contaminated bearings may not show significant signs of failure, but one may want to replace them as a preventative measure.

The geometry of a bearing has an influence on the fundamental fault frequencies. NIS 6205 deep groove ball bearings are used and the geometrical properties are listed Table 1. The idler's rotational speed was kept constant throughout the tests with as little variations as possible. This was done by rotating the drive pulley at 60 RPM with a variable speed drive which translated to an idler speed of 311 RPM, or rotational frequency of 5.183 Hz.

With the idler shaft being stationary, the bearing's inner raceway was also stationary and suitable equations were used to calculate the different fundamental fault frequencies. Assuming no slip, the rolling element pass frequency on the outer and inner raceways, f_{outer} and f_{inner} and the rolling element spin frequency f_{roll} were calculated by equations 3 to 5 respectively (Norton & Karczub, 2003).

$$f_{outer} = Zf_s\left[1 - 0.5\left(1 + \frac{d}{D}\cos(\theta)\right)\right] \quad \text{(Eq. 3)}$$

$$f_{inner} = \frac{Zf_s}{2}\left[1 + \frac{d}{D}\cos(\theta)\right] \quad \text{(Eq. 4)}$$

$$f_{roll} = f_s\left(\frac{D}{d}\right)\left[1 - \left(\frac{d}{D}\cos(\theta)\right)^2\right] \quad \text{(Eq. 5)}$$

The fundamental fault frequencies at the operating speed were calculated and tabulated in Table 2. The accelerometer was attached to the stationary idler shaft as seen in Figure 9 and the test bench operated at a constant speed while interchanging the closest bearing with different fault cases. The measured fault frequencies are tabulated in Table 2 as well as the difference between the calculated and measured frequencies. From the transmissibility test results it can be expected that the bearing frequencies should be transmitted clear enough through the belt.

Figure 13 compares moving averages of one of each of the five different bearing conditions to illustrate differences between the signals. Each bearing condition has a unique frequency spectrum and it was these differences that were used to distinguish the one condition from the other. Although only one signal is shown per bearing fault, many more were obtained and were used in the identification and classification process. As the rolling element impacted the inner and outer race fault, it increased the amplitude of the vibration signal. This can be seen where the amplitude of the spectra of the various fault signals are larger at the frequency corresponding to that fault. A

frequency corresponded to the rolling element fundamental frequency was observed in the rolling defect signal as well as the contaminated bearing. The classification results are shown in Table 3.

3.5. Measuring idler vibrations on the belt

There is reason to believe that the lateral positioning of the accelerometer on the belt may influence the results observed. To investigate this the accelerometer was placed at three different lateral positions on the belt: near the faulty bearing, in the middle of the belt and over the healthy bearing on the far side from the faulty bearing. These positions can be seen Figure 14.

Figure 15 shows the moving averages of the five different bearing conditions as measured near the faulty bearing. As when the measurements were taken on the shaft, similar differences between the healthy bearing and the various faulty bearings can be seen, and it was these differences that were used to identify and classify the bearing faults. There was very little difference between the signals regardless of the lateral position where the measurements were taken on the belt, but the signals measured on the belt differed from the measurements taken on the shaft.

When the accelerometer was attached to the stationary shaft, the excitation frequencies corresponded very well to the calculated fault frequencies. When the accelerometer was attached to the belt, these frequencies did change somewhat as is seen in Figure 15. This seems to indicate significant non-linear behaviour of the system. While the spectra of the vibration measured on the belt superficially appear similar to those measured on the shaft, the measured response no longer correspond well to the calculated source frequencies. This is an important observation which deserves further investigation. However, it is known (Moon & Wickert, 1997) that rubber conveyors belt behave non-linearly, especially if drive speed is not constant.

To explore this further, high-speed footage of the conveyor test bench was recorded and motion amplification was done on the video. From the video it can clearly be seen that the system and the belt in particular behaves in a non-linear way as described in (Zhang & Zui, 1998) and (Kim & Lee, 1999).

The system displayed belt hop between the pulleys and the idler and other characteristics that correspond to the observations, analysis and modelling done of non-linear belt systems by (Zhang & Zui, 1998) and (Kim & Lee, 1999). Non-linear vibration systems have been investigated by (Narayanan & Jayaraman, 1991) and (Choi & Noah, 1988), and it was found that non-linear systems can have subharmonic, superharmonic and chaotic responses to harmonic excitation. This shows that the fundamental fault frequencies as measured on the belt can appear at higher or lower frequencies due to the non-linearity of the on-belt monitoring system and still capture the underlying bearing fault data.

After the measurements were taken on the belt, a plastic container was filled with rocks that covered the accelerometer as seen in Figure 16. A locking lid was placed on top to contain the rocks. The addition of rocks was to more closely approximate realistic conditions that can be found on a conveyor and added much more noise to the signals. Figure 17 shows a comparison between two cases; one with no rocks and the other with the container full of rocks. It is clear that there is a difference between the two signals, especially in the higher frequency range. The fundamental fault frequencies are still distinguishable, but there is much more noise in the signals.

All data sets were pre-processed and the cases treated separately. For each case of sensor placement, the data sets were divided into two equal groups; the training set and the testing set. The gradient based back propagation neural network and the support vector machine was trained with the training set of each case and then the testing set was used to test the accuracy to identify and classify the faulty bearings. The results can be seen in Table 3.

It was observed in the tests without the rocks that, when placing an accelerometer on the belt, regardless of the position, the bearing faults were classified with 100% accuracy when a support vector machine was used. When a payload with a dynamic aspect was investigated, the rocks tumbling around the sensor did add more noise to the signals, but the bearing faults were still classified with 100% confidence with a support vector machine. The artificial neural network was not as accurate as the support vector machine. As the tests progressed, the neural network became more accurate. The gradual wear and enlargement of the defects could have made it easier for the neural network to identify the fault. The test where the accelerometer was placed far from the faulty bearing was more accurate, but also done after a large number of tests were done. From the tests, it was seen that, when sufficient pre-processing is done, a support vector machine is a very powerful classifier. It is strongly advised to further consider support vector machines for in-belt vibration monitoring systems for conveyor idler bearings with the addition of wavelet package decomposition to pre-process the bearing signals.

Conclusion

Manual inspection with the assistance of thermal cameras and acoustic sensing equipment is used to monitor the condition of the conveyor idlers. These methods are labour intensive because an operator has to walk the length of the conveyor inspecting each idler along the way. In some locations where access to idlers are difficult or dangerous, faulty idlers can be overlooked and not replaced when needed. Equipment such as thermal cameras and acoustic sensing equipment has made it easier to inspect idlers, but it is still a laborious task to perform by permanently employed operators. The use of accelerometers to measure the idlers' vibrations and monitor their conditions enables the implementation of an on-line system. The operators can be updated on the condition of the all the conveyor idlers more regularly and automatically when an on-line system is implemented. This system could reduce the labour cost of inspection and will also eliminate the possibility of human error. Operators would not need to access idlers that are difficult or dangerous to inspect and it would therefore reduce the number of injuries on duty. An automatic monitoring system would allow for well-planned shut-downs because regular records are kept on all the idlers and it would be easy to determine the amount and locations of failing idlers that need to be replaced.

Vibration monitoring has been used successfully to monitor the conditions of idlers by fixing accelerometers to the supporting structure of the conveyor. This method could however only monitor a few idlers with a single accelerometer. Either more accelerometers would have to be installed at regular intervals or an operator would have to move the accelerometer a few meters and measure the conditions of the idlers in its vicinity. It can become expensive if a large number of accelerometers and data acquisitioning equipment have to be installed or operators have to be employed to inspect the idlers along the length of the conveyor with the accelerometers.

To reduce the number of accelerometers needed to monitor all the idler bearings, an investigation was done on the feasibility of attaching an accelerometer to the moving belt. As the accelerometer travelled along the length of the conveyor, it measured the vibrations of all the idlers it passed. Vibration monitoring has been found to be very promising to identify and classify faulty idlers when the accelerometer is installed on top of the moving belt. Making use of wavelet package decomposition for data pre-processing and a support vector machine as a classifier, the idler bearing faults were identified and classified with 100% accuracy, regardless of position on the belt or the presence of a dynamic payload or not.

The non-linear characteristics of the on-belt system changed the dominant frequencies of response to the fundamental bearing fault frequencies. However, although the excitation and response frequencies did not correspond very well to one another, the bearing faults were still identified in the signals and the bearings were classified correctly. It is possible to monitor the conditions of idler bearings with accelerometers attached to the

moving belt. Improvements are needed and the data acquisitioning equipment should be embedded into the belt for protection. While there are still a number of practical issues to resolve, this work demonstrate the potential feasibility of idler bearing condition monitoring, through a transducer that is mounted on top (or in practice inside) a conveyer belt.

References

Bishop, C. M., 2006. *Pattern Recognition and Machine learning.* 1 ed. s.l.:Springer.

Choi, Y. S. & Noah, S. T., 1988. Forced Periodic Vibration of Unsymmetric Piecewise-linear Systems. *Journal of Sound and Vibration,* 121(1), pp. 117-126.

Freeman, V. N., 2010. *Apparatus and method for in-belt conveyor idler condition monitoring.* United States of America, Patent No. 7,673,739 B2.

Goodman Conveyor, n.d. *Idler selection procedure.* [Online]
Available at: http://www.beltmaintenance.com/downloads/idler_selection_procedures.pdf
[Accessed 17 November 2015].

Graney, B. P. & Starry, K., 2012. Rolling Element Bearing Analysis. *Materials Evaluation,* 70(1), pp. 78-85.

Kim, S. K. & Lee, J. M., 1999. Analysis of the non-linear vibration characteristics of a belt-driven system. *Journal of Sound and Vibration,* 5(223), pp. 723-740.

Kinder, 2013. *Belt tracking & conveyor maintenance.* [Online]
Available at: http://www.slideshare.net/kinder13/belt-tracking-conveyor-maintenance
[Accessed 05 October 2015].

Li, W. et al., 2013. Design of Online Monitoring and Fault Diagnosis System for Belt Conveyors Based on Wavelet Packet Decomposition and Support Vector Machine. *Advances in Mechanical Engineering,* Volume 2013, p. 10.

Maras, C., 2013. *Thermal imaging cameras a great tool for predictive maintenance inspections.* [Online]
Available at: http://www.maintworld.com/Applications/Thermal-Imaging-Cameras-a-Great-Tool-for-Predictive-Maintenance-Inspections
[Accessed 2015 October 2015].

Moon, J. & Wickert, J. A., 1997. Non-linear vibration of power transmission belts. *Journal of Sound and Vibration,* 4(200), pp. 419-431.

Narayanan, S. & Jayaraman, K., 1991. Chaotic Vibration in a Non-linear Oscillator With Colomb Damping. *Journal of Sound and Vibration,* 146(1), pp. 17-31.

Norton, M. P. & Karczub, D. G., 2003. *Fundamentals of Noise and Vibration Analysis for Engineers.* 2nd ed. s.l.:Cambridge.

Ocak, H., Loparo, K. A. & Discenzo, F. M., 2007. Online tracking of bearing wear using wavelet packet decomposition and probabilistic modeling: A method for bearing prognostics. *Journal of Sound and Vibration,* Issue 302, pp. 951-961.

SKF, n.d. *SKF idler sound monitor kit.* [Online]
Available at: http://www.skf.com/africa/en/industry-solutions/metals/Processes/upstream-steel-making/conveyors/SKF-idler-sound-monitor-kit.html
[Accessed 05 October 2015].

van Tonder, J., 2002. *Idler monitoring feasibility study 2002,* s.l.: Eskom Resources and Strategy Research Division.

Zhang, L. & Zui, J. W., 1998. Non-linear vibration of viscoelastic moving belts, Part II: Forced vibration analysis. *Journal of Sound and Vibration,* 1(216), pp. 93-105.

Zimroz, R. & Król, R., 2009. Failure analysis of belt conveyor systems for condition monitoring purposes. *Studia i Materiały,* 128(36), pp. 255-270.

Table 1: NIS6205 deep groove bearing properties.

Pitch diameter	D	38.5 mm
Rolling element diameter	d	7.94 mm
Contact angle	θ	20°
Number of rolling elements	Z	9
Idler rotational speed		311 RPM
Idler rotational frequency	f_s	5.183 Hz

Table 2: Bearing fundamental fault frequencies.

Frequency	Calculated	Measured	Difference
f_{outer}	18.97 Hz	18.63 Hz	1.8%
f_{inner}	27.68 Hz	26.79 Hz	3.2%
f_{roll}	48.51 Hz	47.63 Hz	1.8%

Table 3: Intelligent systems classification accuracy.

Summary of Intelligent Systems' accuracies			
Sensor placement	Number of testing data sets	Five-class fault classification	
		Neural network	Support vector machine
Fixed on shaft	36	100%	100%
Near the faulty bearing	1073	58.90%	100%
Middle of belt and bearings	700	75.43%	100%
Far from the faulty bearing	633	79.30%	100%
Middle of belt with payload	601	90.18%	100%

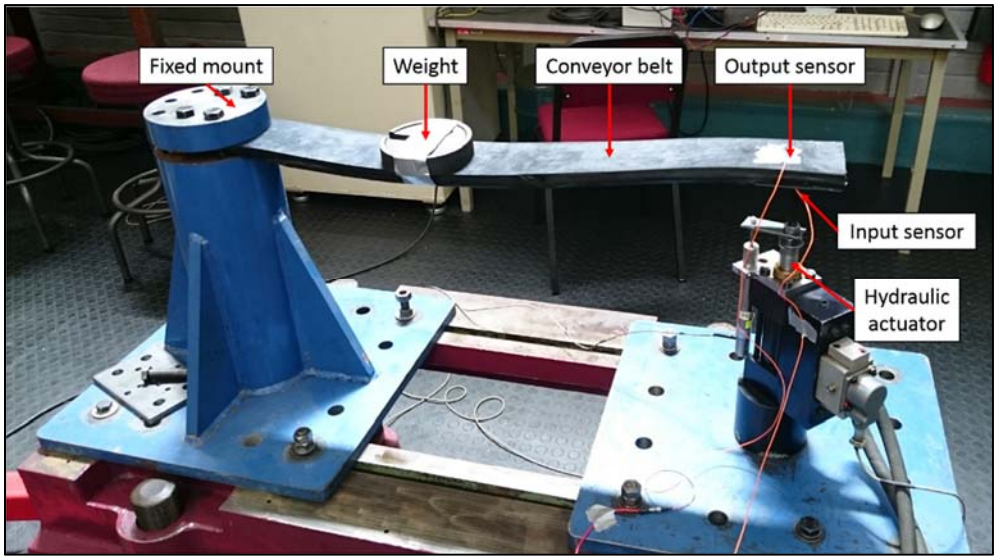

Figure 1: Transmissibility test bench.

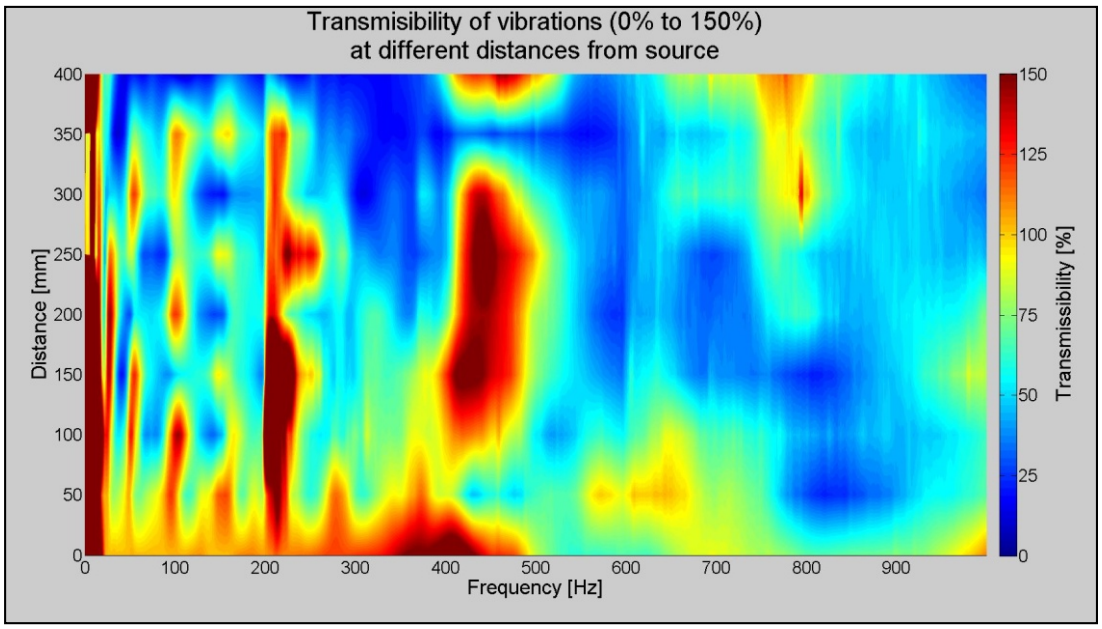

Figure 2: Transmissibility of vibrations through the belt.

Figure 3: Test bench representation of a conveyor.

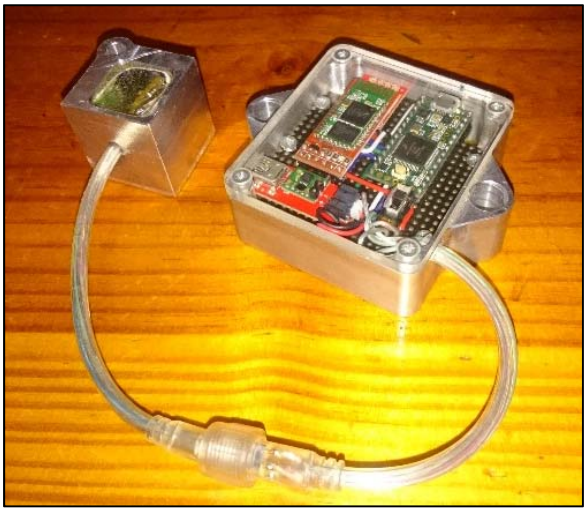

Figure 4: Data logger.

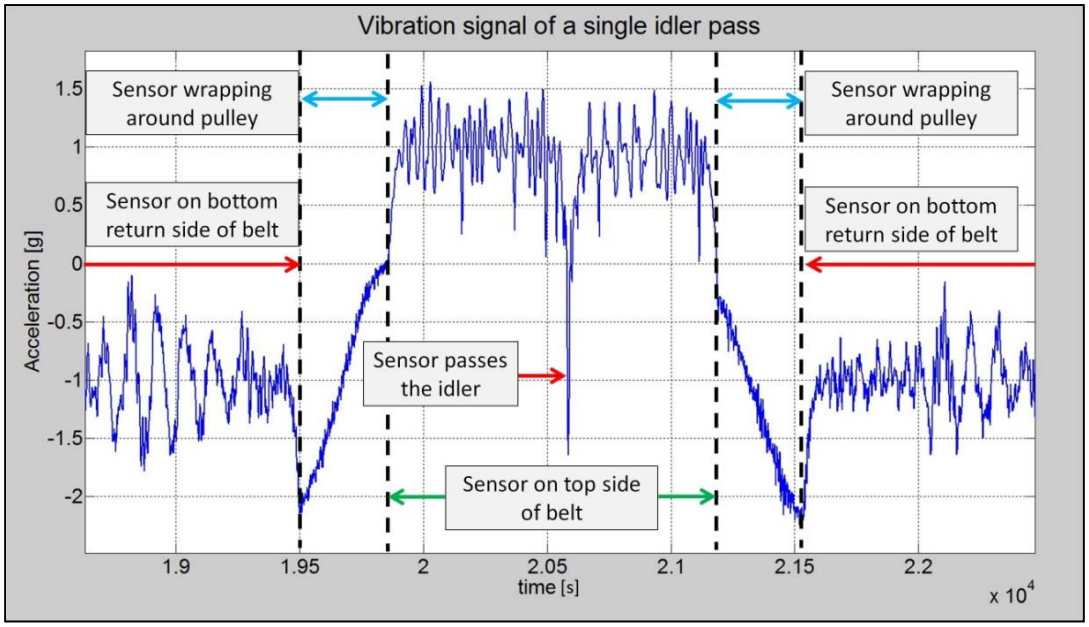

Figure 5: Single idler pass extract.

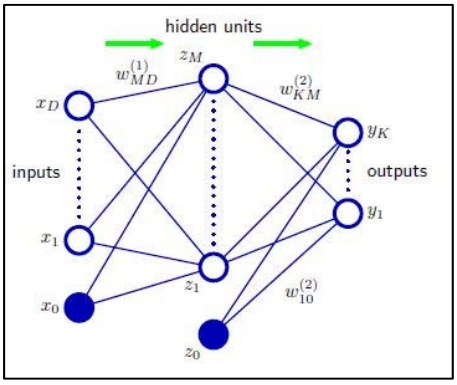

Figure 6: Schematic of a Neural network. (Bishop, 2006)

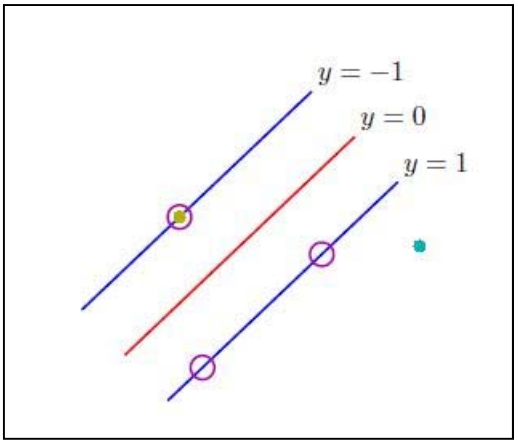

Figure 7: Linear separable data points in feature space. (Bishop, 2006)

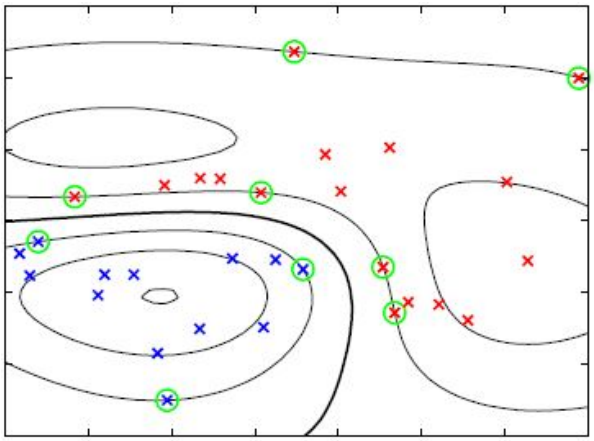

Figure 8: Non-linear classification of data by using a non-linear kernel function. (Bishop, 2006)

Figure 9: Accelerometer attached to idler shaft.

Figure 10: Outer raceway defect.

Figure 11: Inner raceway defect.

Figure 12: Rolling element defect.

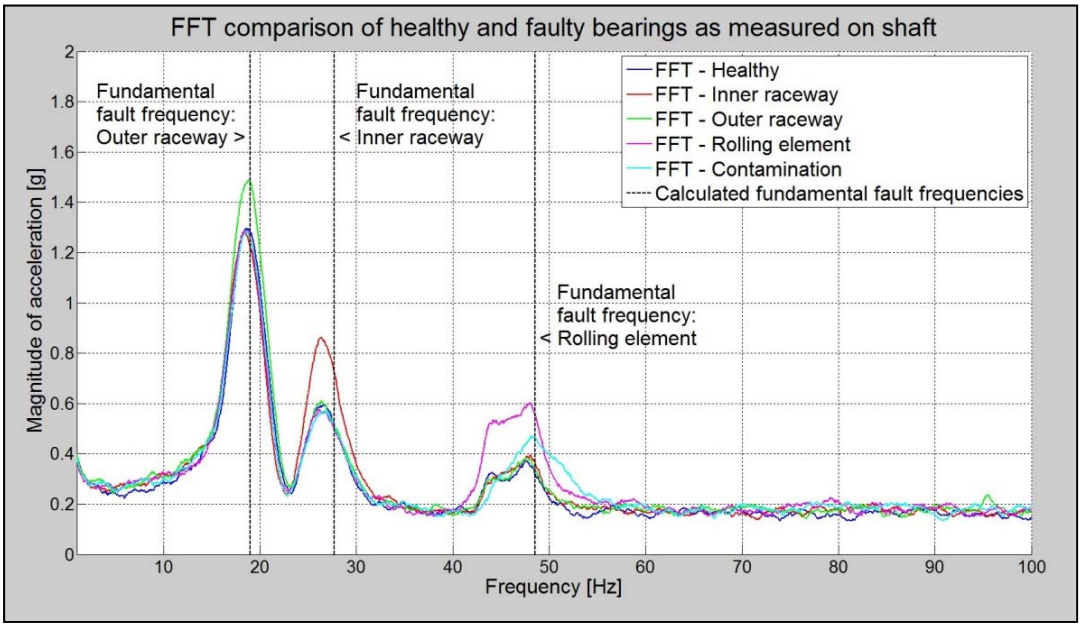

Figure 13: Moving averages for the different bearing conditions as measured on the shaft.

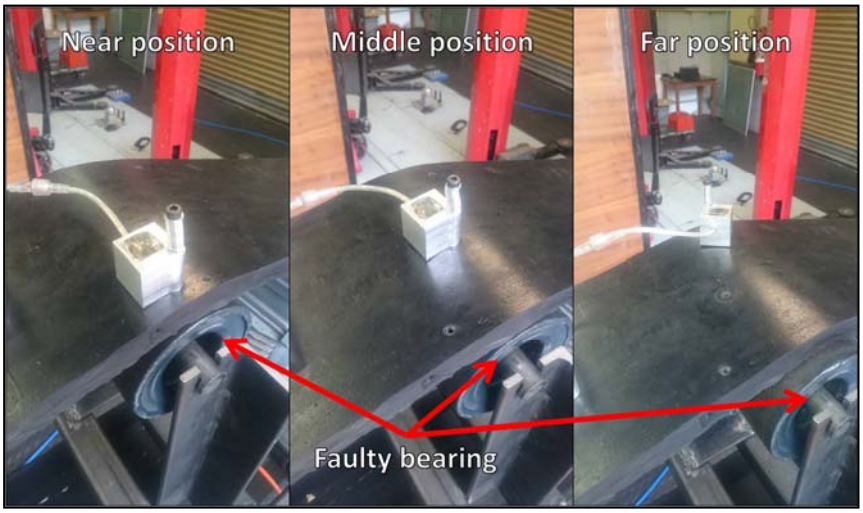

Figure 14: Different sensor positions on the belt.

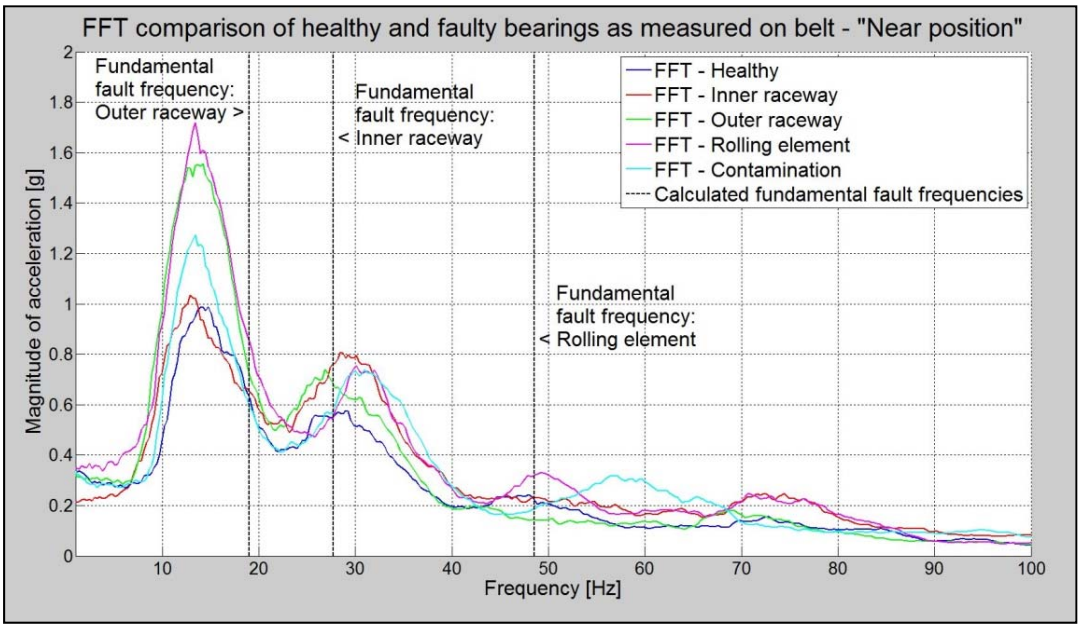

Figure 15: Moving averages for different bearing conditions as measured in the near position.

Figure 16: Payload surrounding the accelerometer.

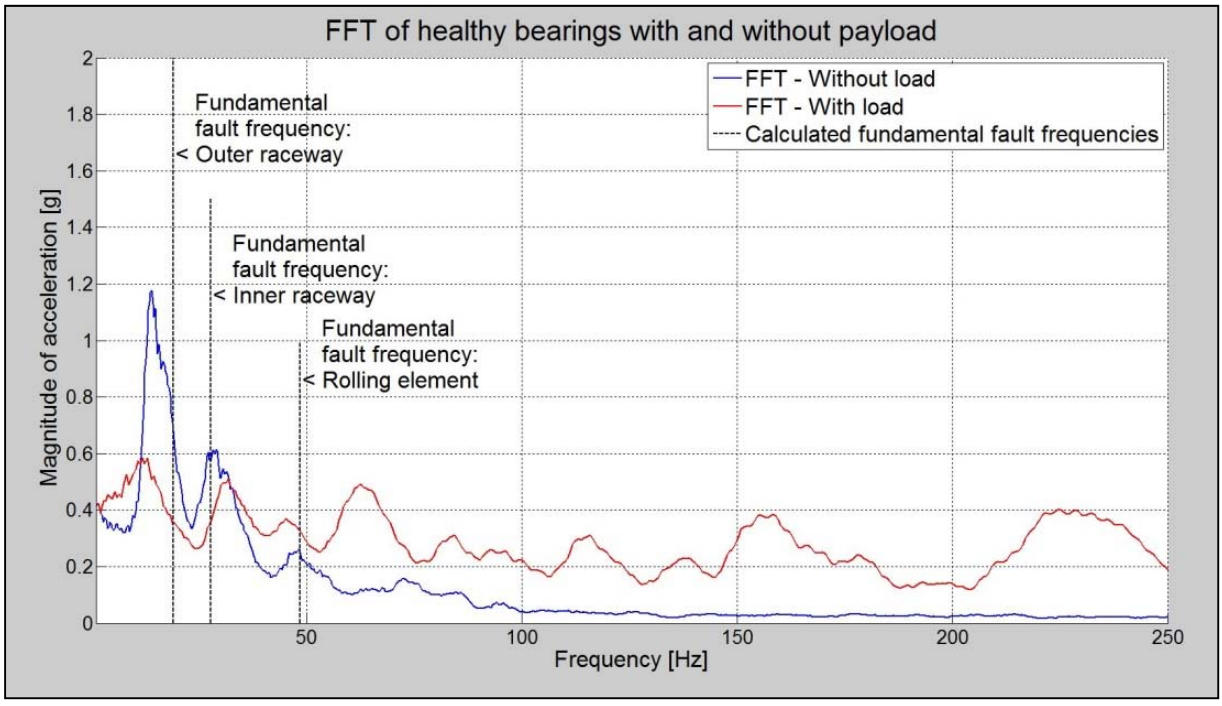

Figure 17: Influence of a payload on the frequency spectrum.